

## Temporal shaping of a heralded single-photon wave packet

So-Young Baek,<sup>\*</sup> Osung Kwon, and Yoon-Ho Kim<sup>†</sup>

*Department of Physics, Pohang University of Science and Technology (POSTECH), Pohang, 790-784, Korea*

(Received 30 July 2007; published 25 January 2008)

We experimentally demonstrate temporal shaping of a heralded single-photon wave packet, prepared by conditional measurement of the idler photon of the entangled photon pair in the process of spontaneous parametric down-conversion. The heralded single-photon wave packet for the signal photon, after being tailored with the help of chirp broadening and interference effects, was observed directly by measuring the time-correlated single-photon-counting histogram. We also demonstrate remote control of the temporal shaping effect by spectral filtering of the idler photon.

DOI: [10.1103/PhysRevA.77.013829](https://doi.org/10.1103/PhysRevA.77.013829)

PACS number(s): 42.65.Lm, 03.65.Ud, 42.25.Bs, 42.81.-i

The single-photon source (SPS) is one of the essential parts that enables photonic quantum-information processing, such as linear optical quantum computing [1], quantum cryptography [2], etc. Currently, there exist a number of competing physical systems to make an efficient SPS [3].

Among these systems, the entangled photon pair generated via spontaneous parametric down conversion (SPDC), combined with a conditional measurement, has long been known as one of the simplest way to prepare a localized single-photon state effectively since its first demonstration in Ref. [4]. Due to the entangled nature of the signal-idler photon pair of SPDC, the detection of the idler photon at the trigger detector nonlocally prepares a well-defined single-photon state, a heralded single-photon state, for the signal photon. A single-photon source of this kind, SPDC SPS, is known to be quite versatile due to the wavelength and bandwidth tunability, the well-defined emission direction, the long-term stability, etc., and, therefore, is now being actively studied and developed for photonic quantum-information-processing applications [5–11].

As with any other optical pulse, the single-photon state must also be associated with a wave packet, which can be loosely defined as the probability distribution of finding a photon within a certain spatiotemporal interval (i.e., the single-photon wave packet is localized) [12–17]. Since quantum interference between independent single photons [18], which is at the heart of physical implementations of photonic quantum-information processing, is affected significantly by the shape of the single-photon wave packet [19], it is of interest and importance to learn how to manipulate and to measure the shape of the single-photon wave packet.

Recently, there have been a few experimental reports on shaping nonclassical wave packets using entangled photon pairs in SPDC [20–22]. Reference [20] reports pulselike biphoton wave packet broadening and Ref. [21] reports modulations within the spectral bandwidth of the biphoton state using a coincidence count measurement. In Ref. [22], temporal shaping of the biphoton state was induced by introducing spectral phase modulation and was demonstrated using the sum frequency generation of the two photons of SPDC as

the two-photon detector. However, temporal shaping and direct time-domain observation of the heralded single-photon wave packet have not been reported to our knowledge.

In this paper, we experimentally demonstrate temporal shaping of a heralded single-photon wave packet using a SPDC SPS. Temporal shaping of the heralded single-photon wave packet was accomplished in a two-step process by using pulselike chirp broadening and interference effects. The wave packet structure in time was then observed directly by measuring the time-correlated single-photon-counting (TCSPC) histogram, synchronized to the detection of the trigger photon, which reveals the temporal probability distribution of the single-photon detection events. We also demonstrate remote control of the temporal shaping of the heralded single-photon wave packet by spectrally filtering the idler photon.

Consider the schematic of the experiment shown in Fig. 1. A 19 mW cw multimode diode laser centered at 408 nm pumps a 3-mm-thick type-I  $\beta$ -barium-borate (BBO) crystal, generating collinearly propagating entangled photon pairs centered at 816 nm. The pump laser was focused at the BBO with a 750 mm lens to increase the single-mode fiber coupling efficiency. A 50-50 beam splitter (BS) splits the collinear signal-idler photon pair spatially. The idler photon is detected by a trigger detector assembly, which consists of a fiber coupler, a 2-m-long single-mode fiber, and an actively quenched single-photon avalanche photodiode (SPAD). IF1 and IF2 are 80 nm full width at half maximum (FWHM) interference filters. IF1 and IF2 are 80 nm full width at half maximum (FWHM) interference filters.

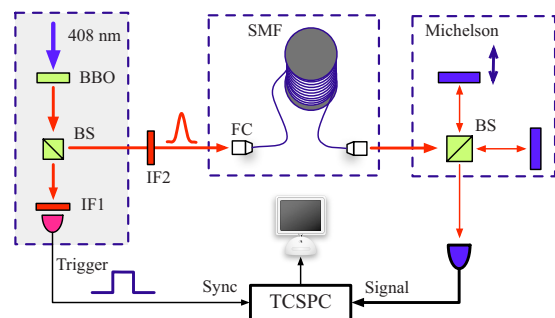


FIG. 1. (Color online) Schematic of the experiment. The heralded single-photon wave packet was prepared by conditional measurement of the idler photon of the SPDC.

<sup>\*</sup>simply@postech.ac.kr

<sup>†</sup>yoonho@postech.ac.kr

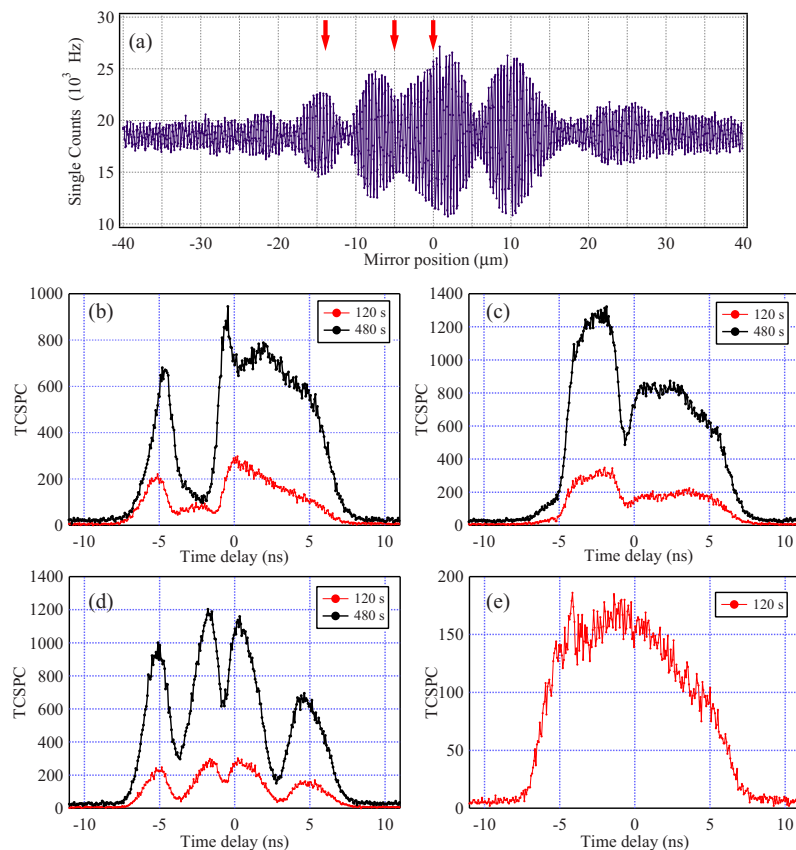


FIG. 2. (Color online) Experimental data. IF1 and IF2 are both 80 nm FWHM filters centered at 816 nm. (a) First-order interference fringe observed at the signal detector. Note that first-order interference provides only information on the spectral bandwidth of the pulse. Red arrows represent the mirror positions where the TCSPC measurements, which reveal the temporal shape of the single-photon wave packet, are taken. Mirror position are (b) 0, (c)  $-5$ , (d)  $-13.5$ , and (e)  $-100$   $\mu\text{m}$ . The red curves with circles (for 120 s) are the lower curves; the black curves with circles (for 480 s) are the upper curves. See text for details.

As mentioned earlier, temporal shaping of the heralded single-photon wave packet for the signal photon is accomplished in a two-step process. The signal photon passes through the interference filter IF2 and is coupled into a 1602-m-long single-mode fiber (SMF) using a fiber coupler (FC). Then the signal photon emerging from the SMF is collimated and sent through a Michelson interferometer with the arm length of approximately 11 cm. The output of the Michelson interferometer is monitored, as a function of the mirror position, with a multimode fiber-coupled SPAD. We record the first-order interference due to the Michelson interferometer as well as the TCSPC (PicoHarp 300, 4 ps minimum resolution) measurement, synchronized to the trigger event, which records the temporal probability distribution of finding a single photon. The TCSPC histogram, therefore, faithfully represents the shape of the heralded single-photon wave packet, provided that the resolution of the TCSPC is much smaller than the wave packet itself. Note that the initial single-photon wave packet, calculated from the measured spectral bandwidth  $\Delta\lambda = 68.9$  nm for the 2-m-long SMF coupled signal and idler photons [23], is found to be subpicoseconds, far beyond the resolution of the single-photon electronics available to date [24]. However, strong chirp broadening of the initial single-photon wave packet due to propagation through the SMF allows us to obtain the wave packet shape directly via the TCSPC measurement [23].

Figure 2 shows the experimental data. In Fig. 2(a), first-order interference of the signal photon is reported. Note that the field autocorrelation by a Michelson interferometer provides only the power spectrum of the light source via the

Wiener-Khinchine theorem, not the temporal profile of the pulse wave packet. The interference envelope shown in Fig. 2(a) exhibits the signature of the well-known  $\text{sinc}^2$ -shaped spectrum of the SPDC photons, albeit with low visibility [25]. The low fringe visibility is not critical for the purpose of this experiment, which is to demonstrate temporal shaping of the single-photon wave packet.

Figures 2(b)–2(d) show the results of the TCSPC measurements, which reveal the wave packet profiles of the signal photon, for several different mirror positions of the Michelson interferometer. For each mirror position of the Michelson interferometer, two TCSPC histograms are taken (at 120 and 480 s). Temporal shaping of the single-photon wave packet is clearly demonstrated in these data.

The experimental data can be understood as follows. When the Michelson interferometer is balanced within the coherence length  $\lambda^2/\Delta\lambda$  of the signal photon [see Figs. 2(b)–Fig. 2(d)] temporal shaping of the single-photon wave packet occurs due to interferometric suppression of specific spectral components in the chirp-broadened single-photon wave packet. Since the effect of the Michelson interferometer can be seen as a sinusoidal spectral filter with a variable frequency  $2\pi/T$ , where  $T$  is the delay between the paths, the wave packet shows more modulation as the Michelson interferometer gets more unbalanced [21]. Moreover, the data show that interferometric shaping of the single-photon wave packet can be practical as the observed wave packet shapes are stable for relatively long accumulation times.

Consider now the case in which the interferometer is made unbalanced by more than the coherence length  $\lambda^2/\Delta\lambda$ ,

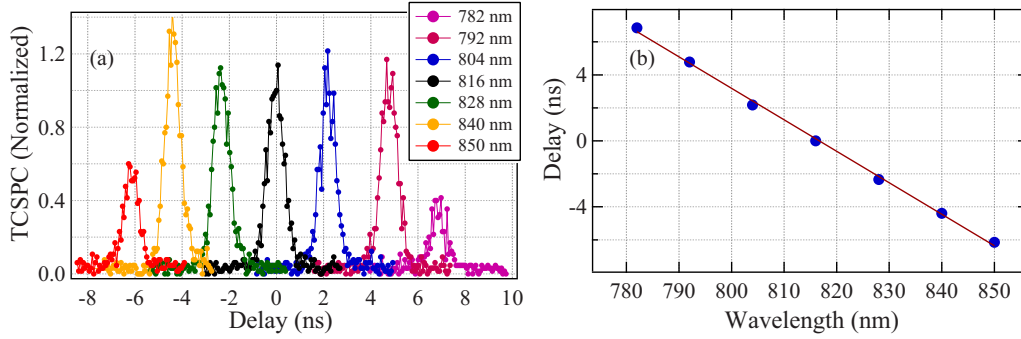


FIG. 3. (Color online) (a) Spectrally and temporally resolved heralded single-photon wave packet, after propagating through a 1602 m single-mode optical fiber. The colored curves with circles given from top to bottom in the legend are shown from right to left in the figure. For this TCSPC measurement, a monochromator with the resolution of 1.5 nm FWHM is used in place of the Michelson interferometer. The data clearly demonstrate that the broadened single-photon wave packet shown in Fig. 2(e) is, in fact, severely chirped. (b) Delay vs wavelength plot for the data shown at left. Solid line is a linear fit to the data.

which is determined by the spectral bandwidth of the signal photon. No interference occurs and, therefore, the TCSPC simply records the chirp-broadened single-photon wave packet due to the 1602-m-long SMF, shown in Fig. 2(e), which is identical to the TCSPC histogram obtained without the Michelson interferometer [23].

Naturally, it is of importance to know which spectral components are actually suppressed in the temporally shaped single-photon wave packets shown in Figs. 2(b)–2(d). To obtain this information, it is necessary to spectrally resolve the chirp-broadened wave packet, such as the one shown in Fig. 2(e). We therefore fed the SMF output directly to a 1/2 m monochromator with a resolution of 1.5 nm. For each wavelength setting of the monochromator, the TCSPC histogram was recorded.

The results are shown in Fig. 3(a) and they clearly demonstrate the chirped nature of the dispersion broadened heralded single-photon wave packet, that is, the redder frequency components appear sooner (negative delay) than the bluer frequency components (positive delay) [23]. In Fig. 3(b), we plot the measured delay (due to group delay dispersion) vs the wavelength data shown in Fig. 3(a). Within the bandwidth of the signal photon, the temporal delay for a specific wavelength component is found to be linearly related to the wavelength for the chirp broadened single-photon wave packet. Since the pulse-broadening mechanism of the SMF does not change in time, Fig. 3(b) can now be used as a reference to which temporally shaped wave packets (due to the Michelson interferometer) can be compared. In other words, the spectral information on the temporally shaped wave packet shown in Fig. 2(b) can be derived easily with the help of Fig. 3(b).

Let us now turn our attention to the remote pulse shaping feature of the experiment. Similarly to a number of recently reported spectral and temporal correlation experiments using SPDC [21–23,26,27], the remote feature in this experiment is based on the fact that the signal-idler photon pair is in the entangled state (hence the remote feature may be made to exhibit nonlocal properties) [25],

$$|\psi\rangle = \int_{-\infty}^{\infty} d\nu S(\nu) |\Omega - \nu\rangle_s |\Omega + \nu\rangle_i, \quad (1)$$

where  $\Omega$  is the central frequency of the SPDC photons, i.e., twice the pump frequency, and  $\nu$  is the detuning frequency. The state  $|\Omega - \nu\rangle_s$  denotes  $a_s^\dagger(\Omega - \nu)|0\rangle$ , where  $a_s^\dagger(\Omega - \nu)$  refers to the creation operator for the signal photon of frequency  $\Omega - \nu$ . The joint spectrum function  $S(\nu)$  for type-I SPDC, which determines the spectral properties of the signal-idler photon pair, is given as  $S(\nu) = \text{sinc}(\nu^2 D'' L / 2)$ , where  $D'' = d^2 k / d\Omega^2$  with  $k \equiv k_s = k_i$ . The subscripts  $s$  ( $i$ ) refers to the signal (idler) photons. Here, we have assumed that the SPDC process is cw pumped.

Given the two-photon entangled pure state in Eq. (1), the quantum states for the signal and the idler photons alone can be calculated as  $\rho_s = \text{Tr}_i(|\psi\rangle\langle\psi|)$  and  $\rho_i = \text{Tr}_s(|\psi\rangle\langle\psi|)$ , respectively, by performing the partial traces of the two-photon density matrix  $|\psi\rangle\langle\psi|$ . If we now include spectral filtering, the quantum state of the signal photon alone, for example, can be written as [25]

$$\rho_s = \int d\nu |S(\nu)|^2 F_s(\nu) |\Omega - \nu\rangle_{ss} \langle\Omega - \nu|, \quad (2)$$

where  $F_s(\nu)$  is the filter function for IF2. The quantum state  $\rho_i$  for the idler photon alone can be expressed in a similar form but with the filter function  $F_i(\nu)$ . Note that the quantum states for the signal and the idler photon alone are completely determined by local parameters. It is also important to emphasize that the signal and the idler photons individually are in thermal (mixed) states, i.e.,  $\rho_{s,i}^2 \neq \rho_{s,i}$ , while the two-photon state of SPDC is a pure state [28]. In other words, Eq. (2) does not represent a single-photon state.

On the other hand, the heralded single-photon state for the signal photon, triggered by the detection event of the idler photon, which is filtered by a narrowband filter IF1, must be described as

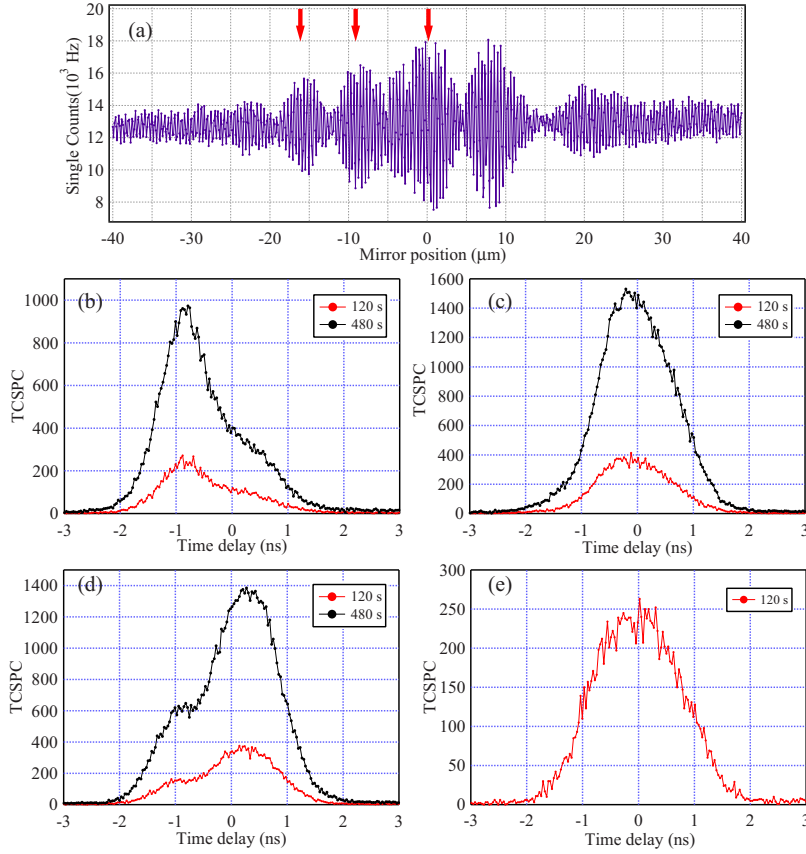


FIG. 4. (Color online) Experimental data. IF1 and IF2 are 10 and 80 nm FWHM filters, respectively. (a) First-order interference fringe observed at the signal detector. The interference pattern is identical to Fig. 2(a). Red arrows represent the mirror positions where the TCSPC measurements are taken. Mirror position are (b) 0, (c)  $-9$ , (d)  $-16$ , and (e)  $-100$   $\mu\text{m}$ . The red and black curves with circles (for 120 and 480 s, respectively) are shown as lower and upper curves in the figure. Note that, compared to Fig. 2, the wave packets are narrower and interference structures are not clearly visible.

$$\rho_s^h = \text{Tr}_i(|\psi\rangle\langle\psi|M_i), \quad (3)$$

where  $M_i$  is the measurement operator for the idler trigger photon. Physically,  $M_i$  represents the ensemble of states of the idler trigger photon at the trigger detector. Since the ensemble of the trigger states is determined by the filtering elements in front of the trigger detector,  $M_i = \int d\omega F_i(\omega)|\omega\rangle\langle\omega|$ , where  $F_i(\omega)$  is the transmission function of the interference filter IF1.

Equation (3), therefore, shows that the bandwidth of the heralded single-photon state  $\rho_s^h$  for the signal photon is remotely (and potentially nonlocally) determined by the bandwidth of the interference filter (IF1) placed in front of the trigger detector [21,23,26]. Choosing a narrower-bandwidth interference filter IF1 for the idler photon, therefore, will affect chirp broadening as well as temporal shaping of the heralded single-photon wave packet for the signal photon.

To demonstrate this effect, we chose an 10 nm FWHM IF1 for the idler photon and an 80 nm FWHM filter IF2 for the signal photon. Since  $\rho_s$  is affected only by local parameters, first-order interference observed at the output of the Michelson interferometer remains unchanged; see Figs. 2(a) and 4(a). However, due to the use of a narrower 10 nm FWHM filter for IF1, the heralded single-photon state  $\rho_s^h$  now has narrower initial bandwidth. As a consequence, the single-photon wave packet will not chirp broaden as much, and this will affect temporal shaping of the heralded single-photon wave packet.

The experimentally measured single-photon wave packets under this condition, for several different mirror positions of the Michelson interferometer, are reported in Figs. 4(b)–4(d). It is clear that temporal shaping of the heralded single-photon wave packet for the signal photon is much reduced or almost disappears due to narrowband filtering of the idler trigger photon.

It is interesting to note that  $\rho_s^h$  generally represents a mixed state unless  $F_i(\omega)$  is infinitely narrow. Recently it has been shown theoretically that it is possible to generate a pure heralded single-photon state without using an infinitely narrowband idler filter by spectrally engineering  $S(\nu)$ , the SPDC two-photon joint spectrum function [9,11]. We are currently developing methods to characterize the pure state heralded single-photon wave packet to study its temporal dynamics.

We have experimentally demonstrated temporal shaping of the heralded single-photon wave packet using chirp broadening and interference effects. Note that the pulse shaping scheme discussed in this paper does not allow precise phase control, which is also important in pulse shaping. We have also demonstrated remote pulse shaping of the heralded single-photon wave packet. The remote pulse shaping feature demonstrated in this experiment could be made even more interesting by relocating the Michelson interferometer into the path of the idler trigger photon and by strictly imposing the nonlocality condition.

The temporally shaped heralded single-photon wave packet can be compressed in time using the chirped-pulse compression method based on the use of a grating pair for



controlling Shih-Alley or Hong-Ou-Mandel-type two-photon quantum interference [29]. Optimal control of such second-order photon-photon interference is essential for implementing many photonic quantum-information protocols [19]. We therefore believe that the single-photon wave packet shaping reported in this paper, combined with the well-known pulse compression technique, should have applications in quantum

optics and photonic quantum-information research, where second-order photon-photon interference effects are utilized.

This work was supported, in part, by the Korea Research Foundation (Grants No. KRF-2005-015-C00116 and No. KRF-2006-312-C00551) and the Korea Science and Engineering Foundation Grant No. (R01-2006-000-10354-0).

- 
- [1] E. Knill, R. LaFlamme, and G. J. Milburn, *Nature (London)* **409**, 46 (2001).
- [2] N. Gisin *et al.*, *Rev. Mod. Phys.* **74**, 145 (2002).
- [3] B. Lounis and M. Orrit, *Rep. Prog. Phys.* **68**, 1129 (2005).
- [4] C. K. Hong and L. Mandel, *Phys. Rev. Lett.* **56**, 58 (1986).
- [5] T. B. Pittman, B. C. Jacobs, and J. D. Franson, *Phys. Rev. A* **66**, 042303 (2002).
- [6] Y.-H. Kim, *Phys. Rev. A* **67**, 040301(R) (2003).
- [7] S. Takeuchi, R. Okamoto, and K. Sasaki, *Appl. Opt.* **43**, 5708 (2004).
- [8] E. Jeffrey, N. A. Peters, and P. G. Kwiat, *New J. Phys.* **6**, 100 (2004).
- [9] M. G. Raymer, J. Noh, K. Banaszek, and I. A. Walmsley, *Phys. Rev. A* **72**, 023825 (2005).
- [10] A. T. Joseph *et al.*, *New J. Phys.* **8**, 91 (2006).
- [11] A. B. U'Ren, Y. Jeronimo-Moreno, and H. Garcia-Gracia, *Phys. Rev. A* **75**, 023810 (2007).
- [12] Note that a space-time-localized wave packet is due to phase coherence or interference among many Fourier (i.e., frequency) components.
- [13] J. E. Sipe, *Phys. Rev. A* **52**, 1875 (1995).
- [14] C. Adlard, E. R. Pike, and S. Sarkar, *Phys. Rev. Lett.* **79**, 1585 (1997).
- [15] I. Bialynicki-Birula, *Phys. Rev. Lett.* **80**, 5247 (1998).
- [16] K. W. Chan, C. K. Law, and J. H. Eberly, *Phys. Rev. Lett.* **88**, 100402 (2002).
- [17] O. Keller, *Phys. Rep.* **411**, 1 (2005).
- [18] C. K. Hong, Z. Y. Ou, and L. Mandel, *Phys. Rev. Lett.* **59**, 2044 (1987).
- [19] P. P. Rohde, T. C. Ralph, and M. A. Nielsen, *Phys. Rev. A* **72**, 052332 (2005).
- [20] A. Valencia, M. V. Chekhova, A. Trifonov, and Y. Shih, *Phys. Rev. Lett.* **88**, 183601 (2002).
- [21] M. Bellini, F. Marin, S. Viciani, A. Zavatta, and F. T. Arecchi, *Phys. Rev. Lett.* **90**, 043602 (2003).
- [22] A. Pe'er, B. Dayan, A. A. Friesem, and Y. Silberberg, *Phys. Rev. Lett.* **94**, 073601 (2005).
- [23] S. Y. Baek, O. Kwon, and Y.-H. Kim (unpublished).
- [24] Assuming a Fourier-transform-limited Gaussian with the time-bandwidth product of  $\Delta t \Delta f = 0.441$ , the FWHM of the initial single-photon wave packet is 14.2 fs.
- [25] Y.-H. Kim, *J. Opt. Soc. Am. B* **20**, 1959 (2003).
- [26] G. Scarcelli *et al.*, *Appl. Phys. Lett.* **83**, 5560 (2003).
- [27] A. Valencia, G. Scarcelli, and Y. Shih, *Appl. Phys. Lett.* **85**, 2655 (2004).
- [28] D. V. Strekalov, Y.-H. Kim, and Y. Shih, *Phys. Rev. A* **60**, 2685 (1999).
- [29] M. Hendrych, M. Micuda, and J. P. Torres, *Opt. Lett.* **32**, 2339 (2007).